

# Mass attenuation Coefficient and Total cross-section Area of Platinum Group Composition

<sup>1</sup>Santosh Kumar Das, <sup>2</sup>Saddam Husain Dhobi

<sup>1</sup>Department of Physics, Patan Multiple Campus, Tribhuvan University, Patandhoka, Lalitpur, Nepal

<sup>2</sup>Physical Science Unit, Nepal Academy of Science and Technology, Khumaltar, Lalitpur Nepal

Email: saddam@ran.edu.np / dassantosh29@gmail.com

Doi: <https://doi.org/10.3126/ppj.v3i2.66188>

## Abstract:

Radiation shielding is a critical practice involving the utilization of materials or barriers to safeguard against ionizing radiation by absorbing, scattering, or blocking the radiation. Its primary objective is to curtail exposure and mitigate potential health risks associated with radiation. In diverse fields like medicine, industry, and nuclear applications, radiation shielding materials play a pivotal role in ensuring the safety of individuals and equipment, contributing significantly to the maintenance of secure environments. This study focuses on characterizing materials for radiation shielding, particularly of Platinum group alloys in varying compositions with hydrogen. Using the Klein-Nishina (KN) formula, the investigation calculates electronic cross-sections (ECS), total mixture cross-section (TMCS), and mass attenuation coefficient (MAC) for different weight percentages of Platinum group alloys (0.1 to 0.6) when exposed to  $\gamma$ -ray photons of various energies. The outcomes emphasize the strong dependence of these cross-sections and MAC on photon energy and the charge number of the material, revealing a decrease with increasing photon energy and an increase with the charge number to mass number ratio ( $Z/A$ ). The research underscores that fundamental parameters such as charge number, photon energy, and  $Z/A$  can be manipulated to enhance the utility of these elements in radiation shielding, protection, dose measurements, and imaging. The study's implications extend to the optimization of Platinum Group alloy compositions, offering insights for the development of tailored materials with enhanced shielding effectiveness in radiation protection and safety applications.

**Keywords:** Radiation Shielding, Klein-Nishina, Electronic Cross-section, Mixture cross-section, mass attenuation coefficient, Platinum Group elements

## Introduction

Gamma rays constitute electromagnetic radiation characterized by very short wavelengths (approximately  $10^{-3}\text{\AA}$  to  $1\text{\AA}$ ), devoid of electric charge, making them impervious to deflection by electric and magnetic fields. Traditional magnetic spectrographs are ill-suited for precisely measuring  $\gamma$ -ray energies due to these properties. Unlike charged particles such as  $\alpha$  and  $\beta$ -rays,  $\gamma$ -radiations possess exceptional penetrating capabilities, lacking a defined range but exhibiting exponential intensity reduction as they traverse absorbing materials (Tayal et al., 2012). In the context of nuclear reactions, the cross-section serves as a measure of the likelihood that a bombarding particle will interact with the target nucleus. This

likelihood is envisioned in terms of the area presented by the nucleus to the incident particle. If the incident particle strikes this area, interaction with the target nucleus occurs; otherwise, it escapes interaction. Thus, a larger cross-section implies a higher probability of a nuclear reaction occurring. It's important to note that the nuclear cross-section is not a geometric representation of the nucleus's area but rather depends on the nature of the interaction process (Ghoshal, 2014). In the realm of gamma ray studies, the linear and mass attenuation coefficients emerge as pivotal parameters, crucial for understanding the interaction between gamma rays and materials. These coefficients are profoundly influenced by the physical state and composition of the material under consideration. Various factors such as the energy of incident gamma radiation, atomic number, density of elements in the shielding material, and the thickness of the shielding play integral roles in determining a material's efficacy in blocking gamma rays (Sallam et al., 2021). The mass attenuation coefficient specifically quantifies the probability of interaction between incident photons and the matter, expressed as the unit mass per unit area. Understanding the mass attenuation coefficients of X and  $\gamma$ -rays in biological and other essential materials holds paramount significance across diverse applications, encompassing industrial, biological, agricultural, and medical domains. Furthermore, the mass attenuation coefficient serves as a valuable tool, offering a wealth of information about the fundamental properties of matter at the atomic and molecular levels. In essence, these coefficients not only provide insights into how well a material can attenuate gamma rays but also contribute to a deeper understanding of the inherent characteristics of materials, making them indispensable for a broad spectrum of scientific and applied disciplines.

Mediums undergo fundamental photon interactions, including the photoelectric effect, Compton scattering, pair production, Rayleigh scattering, and photonuclear processes when exposed to X-/gamma rays. The primary interactions, driven by their interaction cross-sections, are the photoelectric effect, Compton scattering, and pair production, each prevailing in distinct energy ranges. Specifically, Compton scattering dominates in the energy spectrum of radioactive elements and certain radiation facilities utilized for diagnostic and therapeutic purposes in healthcare, ranging from 0.5 MeV to 10 MeV (Büyükyıldız, 2023). The KN theory, rooted in the free electron approximation of the Compton scattering cross-section, stands as a precise method for calculating scattering cross-sections applicable to various elements and materials. Parameters such as scattering cross-sections and attenuation coefficients, including Compton mass attenuation coefficients (CMAC), hold significant importance in accurately determining dosage and various applications in radiation (Alexander et al., 2020).

**Objectives:** The objects of this work are to study the ECS, MCS and MAC of Platinum group-based mixture with hydrogen using Klein-Nishina formula (needed to add formula along with Klein-Nishina).

### Significant of research

This investigation is pivotal for characterizing platinum group metals, including platinum, palladium, and rhodium, offering valuable insights into their radiation attenuation

properties. The findings are particularly relevant for applications such as radiation shielding in nuclear facilities, optimization of medical imaging and therapy utilizing these elements, and advancements in industrial processes where platinum group metals are employed. Additionally, the research contributes to the fields of nuclear science and engineering, aiding in reactor design and fuel analysis, while also offering insights for environmental monitoring and scientific understanding of how these materials interact with radiation. Also, research findings can directly impact the performance and durability of fuel cells by providing insights into how platinum group metals interact with radiation and other environmental factors. This knowledge is instrumental in advancing fuel cell technology, contributing to the development of more efficient and cost-effective energy conversion systems that rely on platinum-based catalysts. The implications of this research extend beyond basic material characterization, offering practical benefits for the sustainable development and widespread adoption of fuel cell technologies.

### Research Methodology

The investigation into X-ray attenuation within metals, specifically aluminum (Al-13), copper (Cu-29), and zirconium (Zr-40), yielded noteworthy results. The study introduced a novel concept to elucidate X-ray scattering, emphasizing the influence of valence and bound electrons (electron distribution) in metals. Surprisingly, for a specific energy range, metals with a higher count of bound electrons in their outermost shell exhibited increased radiation scattering, even when possessing a lower atomic number. When an X-ray beam interacts with an atomic target, two predominant processes unfold: the beam may be absorbed, leading to the ejection of electrons from the atoms, or it may undergo scattering (Warren, 2021). The loss of intensity experienced by incident X-rays passing through a substance is termed attenuation. Numerous experimental and theoretical investigations have delved into exploring the relationship between the attenuation coefficient and the atomic number, encompassing polymers, liquids, crystals, and select metals (Jalal et al., 2023). In the context of  $\gamma$ -ray beams traversing an absorber, attenuation occurs, with the degree of attenuation contingent upon scattering and various absorption processes. The absorption coefficient ( $\mu$ ) is a key parameter derived from the Lambert-Beer law, encapsulating the intricate interplay between  $\gamma$ -ray interactions, absorption, and the atomic structure of the material. This comprehensive exploration of X-ray attenuation in metals provides valuable insights into the nuanced mechanisms governing the interaction of electromagnetic radiation with diverse materials, contributing to the advancement of materials science and related disciplines (Şakar et al., 2020).

$$I = I_0 e^{-\mu t} \quad (1)$$

The expression for the incident  $\gamma$ -ray intensity ( $I_0$ ) in the absence of a sample, the transmitted  $\gamma$ -ray intensity through the sample (I), and the sample thickness (t) in centimeters (cm) and  $\mu/\rho$  signifies the experimental mass-attenuation coefficient of elements.

$$\frac{\mu}{\rho} = \frac{1}{\rho t} \ln \left( \frac{I_0}{I} \right) \quad (2)$$

In the equation, ρ represents the material density in grams per cubic centimeter (g/cm<sup>3</sup>). The theoretical mass-attenuation coefficient μ/ρ (cm<sup>2</sup>/g) for any chemical compound or a combination of elements is determined by the mixture rule as established (Jackson and Hawkes, 1981).

$$\frac{\mu}{\rho} = \sum_i w_i \left( \frac{\mu}{\rho} \right)_i \quad (3)$$

Table 1: Mixture of Platinum group with Hydrogen composition weight

Samples	Pt (A=195.09 amu, Z=78) Composition by weight	Pd (A=106.4, Z=46)	Rh (A=102.90, Z=45)	Ru (A=101.07, Z=44)	H(A=1, Z=1)
S1	0.1	0.1	0.1	0.1	0.6
S2	0.6	0.1	0.1	0.1	0.1
S3	0.1	0.6	0.1	0.1	0.1
S4	0.1	0.1	0.6	0.1	0.1
S5	0.1	0.1	0.1	0.6	0.1

Note: A is atomic mass and Z is atomic number

When discussing KN scattering, the total molecular cross-section (σ<sub>m</sub>) represents the overall likelihood of interaction between incident photons and the entire molecule, accounting for the existence of multiple electrons and their distribution throughout the atomic structure. The relationship between mass attenuation coefficients and total molecular cross-section is expressed as follows, and the mass attenuation coefficients (μ/ρ) values are essential for determining σ<sub>m</sub> (Singh and Gerward, 2002):

$$\sigma_m = \frac{\mu}{\rho} \left( \frac{M}{N_A} \right) \quad (4)$$

Furthermore, in KN scattering, the electronic cross-section (σ<sub>e</sub>) represents the likelihood of contact between an incident photon and a single electron. Specifically, the electronic cross-section measures the probability that a photon would scatter at a given angle and lose energy when interacting with an electron in the setting of Compton scattering, which is explained by the KN formula. The relationship between (μ/ρ) and σ<sub>e</sub> can be written as,

$$\frac{\mu}{\rho} = \frac{\sigma_e Z N_A}{A} \quad (5)$$

Where, M is the molecular weight and N<sub>A</sub> is Avogadro’s number. The predominant scattering mechanism for photons with energy of 511 keV is Compton scattering. In this process, the incident photons interact with an atomic, leading to atomic ionization. The scattering of the incident photon is characterized by an angle θ, which is determined by the Klein-Nishina differential cross-section equation. This equation, as outlined by Dhobi et al. in 2021, provides a mathematical description of how the incident photon scatters at different

angles, offering insights into the Compton scattering phenomenon at this specific photon energy (Dhobi et al., 2021):

$$\left(\frac{d\sigma}{d\Omega}\right)_\alpha = \frac{Zr_e^2}{2} \left(\frac{1}{1+\alpha(1-\cos\theta)}\right)^2 \left( (1+\cos^2\theta) + \frac{\alpha^2(1-\cos\theta)^2}{[1+\alpha(1-\cos\theta)]} \right) \quad (6)$$

The probability of Compton scattering for a single atom when it interacts with light photons is expressed by the KN and is also known as the Klein-Nishina cross-section per atom ( $\sigma_a$ ). The probability that a photon will lose energy when it scatters off a single electron in an atom is measured by the KN cross-section. Additionally, the expression for the KN cross-section per atom is as follows:

$$\sigma_\alpha = 2\pi \int_0^\pi \left(\frac{d\sigma}{d\Omega}\right)_\alpha \sin\theta d\theta \quad (7)$$

Upon solving equations (6) and (7), the comprehensive KN cross-section per atom is derived as follows (Thiele et al., 2021 & Williams et al., 2023):

$$\sigma_\alpha = Z2\pi r_e^2 \left\{ \frac{1+\alpha}{\alpha^2} \left[ \frac{2(1+\alpha)}{1+2\alpha} - \frac{\ln(1+2\alpha)}{\alpha} \right] + \frac{\ln(1+2\alpha)}{2\alpha} - \frac{1+3\alpha}{(1+2\alpha)^2} \right\} \quad (8)$$

where  $r_e = 2.818 \text{ fm}$  is the classical electron radius,  $Z$  is the nuclear charge of the target molecule and  $\alpha = \frac{E}{m_e c^2} = \frac{E}{0.511 \text{ MeV}}$ , for non-relativistic case,  $mc^2 = 0.511 \text{ MeV}$  (MIT, 2013). Since KN atomic cross-sections are obtained by multiplying electronic cross-sections with charge number  $Z$  of each element that is  $\sigma_\alpha = Z \cdot \sigma_e$  and hence, the electronic cross-sectional area is obtained as:

$$\sigma_e = 2\pi r_e^2 \left\{ \frac{1+\alpha}{\alpha^2} \left[ \frac{2(1+\alpha)}{1+2\alpha} - \frac{\ln(1+2\alpha)}{\alpha} \right] + \frac{\ln(1+2\alpha)}{2\alpha} - \frac{1+3\alpha}{(1+2\alpha)^2} \right\} \quad (9)$$

Also, from equation (9) and (5), and using table for different chemical composition we have mass attenuation coefficient is obtained as

$$\left(\frac{\mu}{\rho}\right)_{S1} = 2.31 \times 10^{-5} \left\{ \frac{1+\alpha}{\alpha^2} \left[ \frac{2(1+\alpha)}{1+2\alpha} - \frac{\ln(1+2\alpha)}{\alpha} \right] + \frac{\ln(1+2\alpha)}{2\alpha} - \frac{1+3\alpha}{(1+2\alpha)^2} \right\} \quad (10)$$

$$\left(\frac{\mu}{\rho}\right)_{S2} = 1.41 \times 10^{-5} \left\{ \frac{1+\alpha}{\alpha^2} \left[ \frac{2(1+\alpha)}{1+2\alpha} - \frac{\ln(1+2\alpha)}{\alpha} \right] + \frac{\ln(1+2\alpha)}{2\alpha} - \frac{1+3\alpha}{(1+2\alpha)^2} \right\} \quad (11)$$

$$\left(\frac{\mu}{\rho}\right)_{S3} = 1.46 \times 10^{-5} \left\{ \frac{1+\alpha}{\alpha^2} \left[ \frac{2(1+\alpha)}{1+2\alpha} - \frac{\ln(1+2\alpha)}{\alpha} \right] + \frac{\ln(1+2\alpha)}{2\alpha} - \frac{1+3\alpha}{(1+2\alpha)^2} \right\} \quad (12)$$

$$\left(\frac{\mu}{\rho}\right)_{S4} = 1.47 \times 10^{-5} \left\{ \frac{1+\alpha}{\alpha^2} \left[ \frac{2(1+\alpha)}{1+2\alpha} - \frac{\ln(1+2\alpha)}{\alpha} \right] + \frac{\ln(1+2\alpha)}{2\alpha} - \frac{1+3\alpha}{(1+2\alpha)^2} \right\} \quad (13)$$

$$\left(\frac{\mu}{\rho}\right)_{S5} = 1.46 \times 10^{-5} \left\{ \frac{1+\alpha}{\alpha^2} \left[ \frac{2(1+\alpha)}{1+2\alpha} - \frac{\ln(1+2\alpha)}{\alpha} \right] + \frac{\ln(1+2\alpha)}{2\alpha} - \frac{1+3\alpha}{(1+2\alpha)^2} \right\} \quad (14)$$

The KN cross-section finds crucial applications in radiation shielding, particularly in understanding and designing effective shielding materials. This cross-section is pivotal for assessing the scattering behavior of photons and electrons, providing insights into how materials interact with incident radiation. One significant application lies in optimizing

radiation shielding materials to reduce exposure to ionizing radiation. By considering the KN cross-section, researchers and engineers can tailor materials that effectively attenuate and scatter radiation, thereby enhancing the safety of individuals working in radiation-prone environments.

### **Results and Discussion**

The research utilized a mixture model, incorporating weight percentages, to calculate the ECS, TMCS, and MAC. The computations were carried out using the Online MATLAB student package. The composition values, expressed as weight percentages, were determined and organized in Table 1, providing a comprehensive overview of the material composition. The investigation delved to study the nature of ECS, TMCS, and MAC, exploring their characteristics in response to the variation in incident photon energy. This analysis was visually represented through Figure 1 to Figure 4, illustrating how ECS, TMCS, and MAC change in relation to different incident photon energy levels. The figures 1 to 4 serve as valuable graphical representations, aiding in the understanding of the behavior and trends exhibited by ECS, TMCS, and MAC across the specified range of incident photon energies.

#### **Electronic Cross section**

The ECS behavior of the KN cross-section is depicted in Figure 1. A notable observation from the figure reveals a consistent decrease in ECS with increasing photon incidence energy. Particularly in the X-rays region, the ECS demonstrates a significant elevation, whereas in the gamma region, it exhibits a comparatively lower magnitude. This intriguing trend can be attributed to the fact that, at higher energy levels, photons approach very closely to the electrons of the target atom, rendering the ECS independent of atomic number and mass. Instead, it becomes intricately dependent on the incidence energy of photons. This phenomenon is supported by previous studies (Singh & Gerward, 2002), emphasizing that at elevated photon energies, the interaction between photons and target electrons is primarily governed by their proximity rather than atomic properties. Conversely, in the lower energy region, the ECS is higher, indicating a larger separation between incident photons and target electrons. This phenomenon results in a weaker interaction compared to the higher energy region, where the closer proximity intensifies the interaction. The intricate relationship between ECS and incident photon energy underscores the nuanced nature of electron-photon interactions in the examined material composition.

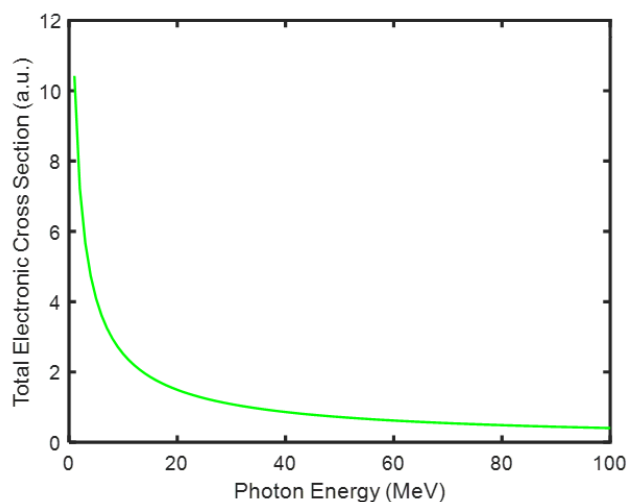


**Figure 1:** KN ECS with incidence energy of photons

The complex interaction between classical and quantum characteristics can be used to explain the decrease in ECS with rising photon incidence energy in KN scattering. Incident photons get very close to the target atom's electrons at increasing photon energy. This can be understood classically as higher-energy photons entering the electron cloud at a deeper level. Higher energy photons have shorter wavelengths according to quantum mechanics, which causes the photon's representation inside the electron cloud to be more limited and localized. Interference effects increase in strength as photons get closer to electrons, affecting the likelihood of a contact. At high photon energies, the photon-target electron interaction is dominated by the photon-proximity effect, where photon-to-target electron interaction is mostly controlled by photon proximity instead of atomic characteristics. Furthermore, in Compton scattering, the observed drop in electronic cross-section is partly explained by the diminished importance of energy transfer at higher energies.

### **Total Mixture cross section**

The TMCS of platinum-group elements with varying compositions of hydrogen is meticulously detailed in Table 1, and its behavior is graphically represented in Figure 2. The examination reveals that the TMCS, akin to ECS, exhibits a discernible trend influenced by the atomic number and atomic weight. Specifically, the TMCS follows an increasing order of  $Pt > Pd > Rh > Ru > H$ . This order suggests that materials with higher atomic numbers and atomic weights tend to have greater TMCS values. This finding contrasts with ECS, where the order was solely dictated by the incidence energy of photons. The comparison with previous work by Dhobi et al. (2021) on the Klein Nishina differential equation for radiation shielding materials emphasizes the nuanced nature of these interactions. Furthermore, the TMCS values are observed to be greater than ECS. This discrepancy arises from the difference in target entities; in ECS, the target is an electron, while in TMCS, the target is a mixture or compound. Additionally, the field of the mixture presents a larger interaction region, in contrast to the lower interaction region in ECS. This comparative

analysis sheds light on the distinct behaviors of ECS and TMCS, underlining the importance of considering both atomic properties and material composition in understanding their respective characteristics.

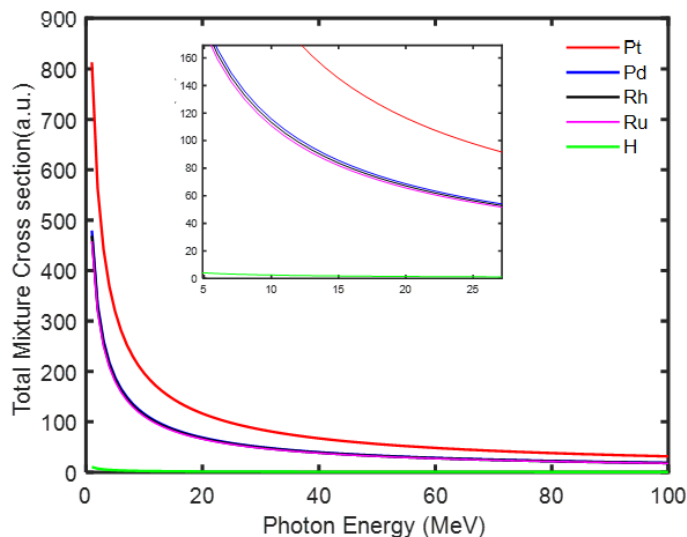


**Figure 2:** KN TMCS with incidence energy of photons

There are several elements that interact complexly to cause the drop in TMCS in KN scattering as photon incidence energy increases. Due to decreased energy transfer in the scattering of Compton and photons' closer proximity to target atom electrons, individual ECS drop at higher photon energies. This electron-proximity influence becomes pronounced and affects the overall properties of scattering. Atomic weight and atomic number also have an impact on the TMCS, which adds to the total scattering likelihood of the material. The observed decline is influenced by changes in atomic characteristics and material composition in addition to photon incidence energy. Understanding the action of TMCS in KN scattering requires taking into account both atomic characteristics and composition, as demonstrated by a subtle relationship revealed by a comparative analysis with ECS.

### Mass attenuation coefficient

In Figure 3, the MAC is depicted, revealing similarities with the TMCS and ECS. The MAC, quantified at an order of  $10^{-5}$  cm<sup>2</sup>/g, is contingent upon factors such as atomic number, atomic mass, and Electron Compton Scattering. Among the examined samples, denoted as S1 through S5, it is observed that S1 exhibits a higher MAC value. This signifies that when incident radiation traverses through S1, the attenuation of photon intensity is more pronounced compared to the other samples. The descending order of MAC values across the samples is established as S1 > S2 > S3 > S4 > S5. This ranking implies that S1 possesses a greater capability to diminish the intensity of incident photons compared to S2, S2 surpasses S3, and so forth. The composition by weight percentage of the samples also influences the MAC. Notably, S2, characterized by a higher weight percentage of Pt elements, exhibits a

lower MAC. Specifically, a composition of 0.6% by weight of Pt, alongside 0.1% by weight of other elements, results in a diminished capacity to reduce the intensity of incident photons. In contrast, the MAC is higher for S1, which comprises 0.6% by weight of Hydrogen and 0.1% by weight of other elements. This indicates that the composition of Hydrogen in S1 has a heightened capacity to reduce the intensity of incident photons compared to the Pt-rich composition in S2. The range of MAC obtained of this finding is also observed (Elmahroug et al., 2015).

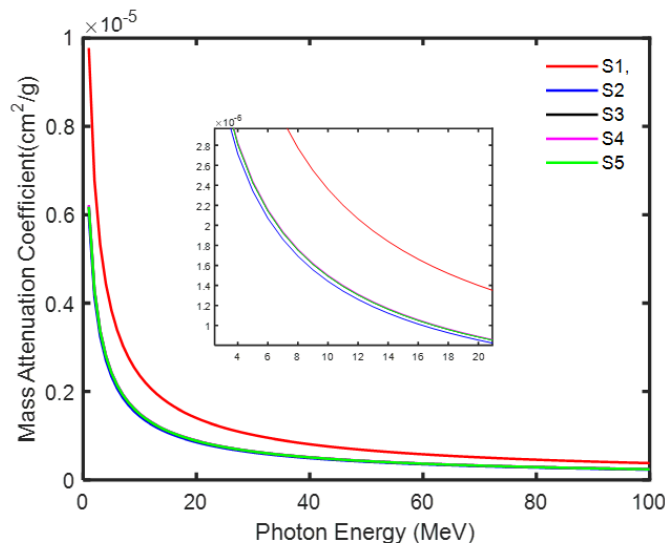


**Figure 3:** Incidence energy of photon vs MAC

The dominant influence of the Compton scattering at higher energies is responsible for the drop in the MAC in KN scattering with increasing incidence photon energy. The energy transmitted in a single Compton scattering incident decreases as high-energy photons interact with the material's electrons. The transmitted photon intensity decreases less as a result of this decreased energy transfer. Shorter wavelengths combined with high-energy photons' close proximity to electrons cause a general drop in MAC. Additionally, the diverse elemental compositions are the source of variances in MAC values between various compositions, such as those designated as S1 through S5. For example, S1, which has a greater weight percent of hydrogen, has a higher MAC than compositions that are rich in Pt, such as S2. The complex interaction between elemental composition, electron-photon proximity effects, as well as energy transfer highlights the varied behavior of MAC with respect to varying incidence photon energies as well as material compositions.

The presence of the Compton scattering at higher energies can explain the MAC decrease with increasing incidence photon energy. The predominant interaction mechanism, Compton scattering, occurs when electrons receive energy from incident photons, which lowers the intensity of photons transmitted. At higher photon energies, when shorter wavelengths lead to a decreased chance of interaction between photons as well as electrons, this loss in energy transfer is most noticeable. Dispersion dynamics are further influenced

and MAC is reduced by the close proximity of high-energy photons to electrons within the material, in addition to interference effects. To put it another way, the material's ability to absorb the energy of the incident photon is diminished as photon energy rises, which is what causes the observed drop in MAC. This knowledge highlights how important it is to take into account Compton scattering dynamics when forecasting a material's attenuation behavior at different photon energy, which is crucial for radiation shielding and dosage predictions.

### Conclusion

Through the use of the mixture model for platinum group alloy including hydrogen, this study offered a thorough comprehension of how ECS, TMCS, and MAC react to changes in incident photon energy. The ECS consistently decreased as photon energy increased, highlighting the complex nature of electron-photon interaction. TMCS defied the trend seen in ECS by exhibiting a unique order affected by atomic characteristics. The MAC, measured at  $10^{-5}$  cm<sup>2</sup>/g, showed sample-dependent ranking (S1>S2>S3>S4>S5), indicating that sample composition affects incident photon attenuation. This study highlights the significance of taking into account both atomic characteristics and the composition of materials in radiation shielding systems and advances our awareness of the complex behaviors of ECS, TMCS, as well as MAC.

### Acknowledgement

The authors would like to express their gratitude to Department of Physics, Patan Multiple Campus, Tribhuvan University, Patandhoka, Lalitpur, Nepal, and Nepal Academy of Science and Technology, Khumaltar, Lalitpur, Nepal, for their invaluable contributions and support in this research endeavor. Their expertise and collaboration have significantly enriched the quality and depth of this work.

Authors contribution: All authors are equally contributed.

### Bibliography

- MIT. (2013). Relativistic Dynamics: The Relations Among Energy, Momentum, and Velocity of Electrons and the Measurement of  $e/m$ . Department of Physics. Retrieved from <http://web.mit.edu/8.13/www/JLEperiments/JLExp09.pdf>
- Dhobi, S. H., Das, S. K., & Yadav, K. (2021). Klein Nishina Differential Equation for the Selection of Radiation Shielding Material (C, AL, Fe, and Zn) on the Basis of Attenuation and Cross-sectional Area. *European Journal of Applied Physics*, **3**(1):31-38.
- Singh, K., & Gerward, L. (2002). Summary of existing information on gamma-ray and X-ray attenuation coefficients of solutions. *Indian Journal of Pure and Applied Physics*, **40**(9): 643–649.
- Şakar, E., Özpolat, Ö.F., Alım, B., Sayyed, M., and Kurudirek M. (2020). Phy-X/PSD: Development of a userfriendly online software for calculation of parameters relevant to radiation shielding and dosimetry. *Radiation Physics and Chemistry*, 108496, 1-12

- Jackson, D. F., & Hawkes, D. J. (1981). X-ray attenuation coefficients of elements and mixtures. *Physics Reports*, **70**(3):169–233.
- Tayal, D. C. (2012). *Nuclear Physics* (6th ed.).
- Ghoshal, S. N. (2014). *Nuclear Physics* (13th ed.).
- Sallam, F. H., Ibrahim, E. M., Hassan, S. F., & Omar, A. (2021). Shielding properties enhancement of bentonite clay nanoparticles coated by polyvinyl alcohol polymer. *Research Square*. <https://doi.org/10.21203/rs.3.rs-645961/v1>.
- Singh, K., & Gerward, L. (2002). Summary of existing information on gamma-ray and X-ray attenuation coefficients of solutions. *Indian Journal of Pure and Applied Physics*, **40**(9): 643–649.
- Jalal, V.J., Tofiq, N.F., Muhammad, S.S. (2023). The Dependence of X-Ray Attenuation Parameters of (Al, Cu, And Zr) Metals on their Atomic Number. *Journal of Studies in Science and Engineering*, **3**(1):54-60. <https://doi.org/10.53898/josse2023314>
- Warren, B. E. (1990). *X-ray Diffraction*. Cour Corp. 381 pages. [https://books.google.iq/books?id=wflBhAbEYAsC&dq=%22X-ray%22&lr=&source=gbs\\_navlinks\\_s](https://books.google.iq/books?id=wflBhAbEYAsC&dq=%22X-ray%22&lr=&source=gbs_navlinks_s) (accessed May 2, 2021).
- Elmahroug, Y., Tellili, B., & Souga, C. (2015). Determination of total mass attenuation coefficients, effective atomic numbers and electron densities for different shielding materials. *Annals of Nuclear Energy*, **75**:268–274. doi:10.1016/j.anucene.2014.08.015
- Büyükıldız, M. (2023). A comparative study on Compton mass attenuation coefficient based on Klein-Nishina theory for different types of materials in the energy range 0.284–15 MeV. *Radiation Physics and Chemistry*, **212**(111137):23-46. <https://doi.org/10.1016/j.radphyschem.2023.111137>
- Alexander, R.W., Thiele, K.T. and Maqbool, M. (2023). Electronic cross-sections and Compton attenuation and transfer coefficients of  $^{82}\text{Pb}208$ ,  $^{29}\text{Cu}64$ ,  $^{27}\text{Co}59$ ,  $^{20}\text{Ca}40$  and  $^{13}\text{Al}27$  for applications in radiation shielding and dose, *PhysicaScripta*. **95**(085006):21-46. DOI 10.1088/1402-4896/ab9e23
- Thiele, K. T., Alexander, R. W., Maqbool, M. (2021). Characterization of  $^{83}\text{Bi}^{209}$ ,  $^{74}\text{W}^{184}$ ,  $^{48}\text{Cd}^{112}$ ,  $^{30}\text{Zn}^{65}$ ,  $^{28}\text{Ni}^{59}$ , and  $^{26}\text{Fe}^{56}$  using the Modified Klein-Nishina formula for radiation shielding and dosimetry. *Radiation Physics and Chemistry*, **179**(109264). <https://doi.org/10.1016/j.radphyschem.2020.109264>
- Williams, K. A., Wright, B. K., Perrigin, M. W., Caffrey, E., Khan, Q., Maqbool, M. (2023). Radiation shielding characterization of  $^{83}\text{Bi}^{209}$ ,  $^{74}\text{W}^{184}$ ,  $^{50}\text{Sn}^{119}$ , ZnS, and  $\text{CaCO}_3$  using the modified Klein-Nishina formula. *Radiation Physics and Chemistry*, **205**(110712):2. <https://doi.org/10.1016/j.radphyschem.2022.110712>